Diffusion Measures of Subcortical Using High-Field MRI

Hyeon-Man Baek[1,2*] and Ji-Yeon Suh[2]

[1]Gachon Advanced Institute for Health Sciences and Technology, Incheon, Korea, [2]Lee Gil Ya Cancer & Diabetes Institute, Gachon University, Incheon, Korea

Background & Introduction

- Deep brain structures such as the subthalamic nucleus and globus pallidus internal have shown to be effective targets of deep brain stimulation in treating Parkinson's Disease [Krause et al., Journal of Neurology, Neurosurgery & Psychiatry 2001].
- Accurate segmentations of deep brain targets ex-vivo is important in providing accurate locations of deep brain targets, as well as for observing effects of Parkinson's disease and deep brain stimulation surgery [Behrens et al., Neuroimage 2007].
- However, popular segmentation toolboxes such as FSL and Freesurfer cannot automatically segment particular deep brain structures, such as STN, RN. Additionally, the same toolboxes cannot segment GPI and GPE separately.
- The intention of this study was to utilize Lead-DBS, an open source toolbox designed to provide precise locations of anatomical structures for deep brain stimulation surgery, to segment subthalamic nucleus (STN), red nucleus (RN), globus pallidus internal (GPI) and globus pallidus external (GPE) [Horn A and Kühn AA, Neuroimage, 2015].
- In addition, we compare the diffusion measures of 3T and 7T mean, whole-brain structural connectome with PPMI normative connectome using x-direction sampling [Marek et al., Progress in neurobiology, 2011; Ewert et al., Neuroimage, 2017].

Materials and Methods

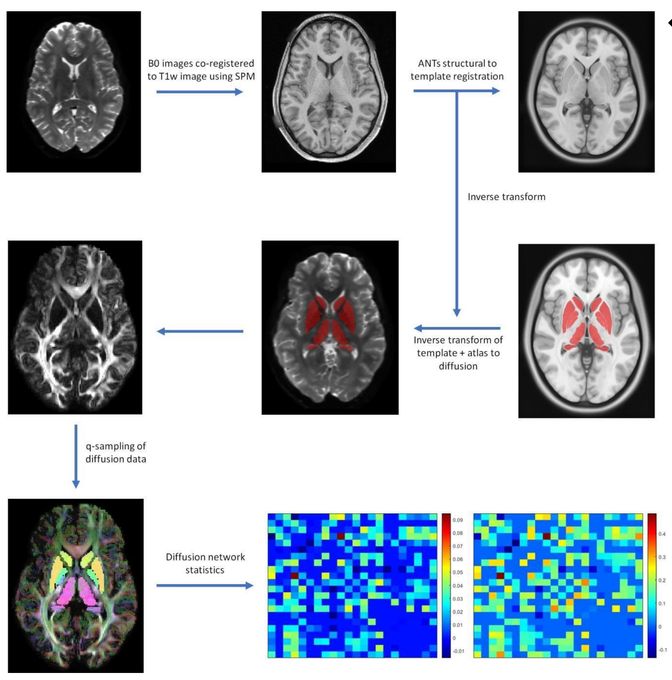

❖ **Figure 1.** Basic processing Lead−connectome pipeline. Minimally preprocessed human connectome project images are co-registered to the structural T1w image using SPM. Structural images are registered to templates using ANTs registration, generating inverse transforms to translate MNI PD25 template to b0 space. DSI Studio is used to apply Q−sampling on diffusion images to reconstruct diffusion orientations and generate diffusion network statistics of segmented ROIs and ROI diffusion connectivity

- Data Analysis performed on preprocessed 3T and 7T T1 and DTI images of four patients obtained from Human Connectome Project (HCP) [Van Essen et al., Neuroimage, 2013].

3T

Parameter	Value
Sequence	Spin-echo EPI
TR	5520 ms
TE	89.5 ms
flip angle	78 deg
refocusing flip angle	160 deg
FOV	210x180 (RO x PE)
matrix	168x144 (RO x PE)
slice thickness	1.25 mm, 111 slices, 1.25 mm isotropic voxels
Multiband factor	3
Echo spacing	0.78 ms
BW	1488 Hz/Px
Phase partial Fourier	6/8
b-values	1000, 2000, and 3000 s/mm2

7T

Parameter	Value
Sequence	Spin-echo EPI
TR	7000 ms
TE	71.2 ms
flip angle	90 deg
refocusing flip angle	180 deg
FOV	210x210 (RO x PE)
matrix	200x200 (RO x PE)
slice thickness	1.05 mm, 132 slices, 1.05 mm isotropic voxels
Multiband factor	2
Image Acceleration factor (iPAT)	3
Echo spacing	0.82 ms
BW	1388 Hz/Px
Phase partial Fourier	6/8
b-values	1000, 2000 s/mm2

- **Lead-DBS** ANTs atlas based segmentation using MNI PD25 atlas [Avants et al., Medical image analysis, 2008; Xiao et al., Data in brief, 2017].
- **DSI Studio and q-sampling** for generating diffusion measures of between each segmented structure [Yeh et al., Neuroimage, 2010].
- **Student-t test** used to determine significant difference with p <0.05; FDR correction with Benjamini-Hochberg procedure

Results (I): Subcortical structure segmentation

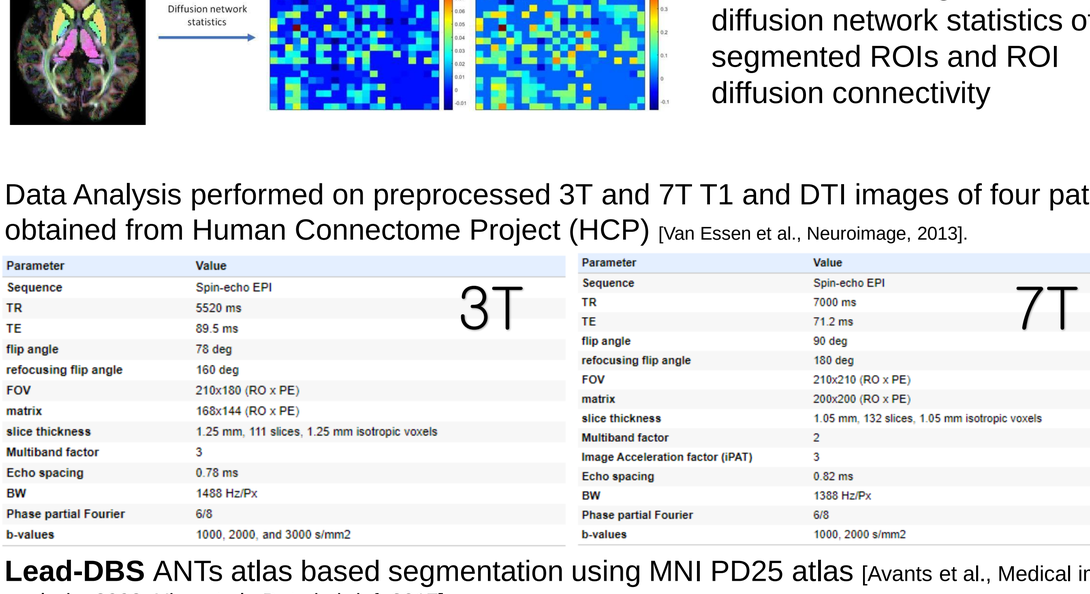

❖ **Figure 2.** Basic processing Lead−connectome pipeline. Minimally preprocessed human connectome project images are co-registered to the structural T1w image using SPM.

Results (II): Subcortical diffusion measures

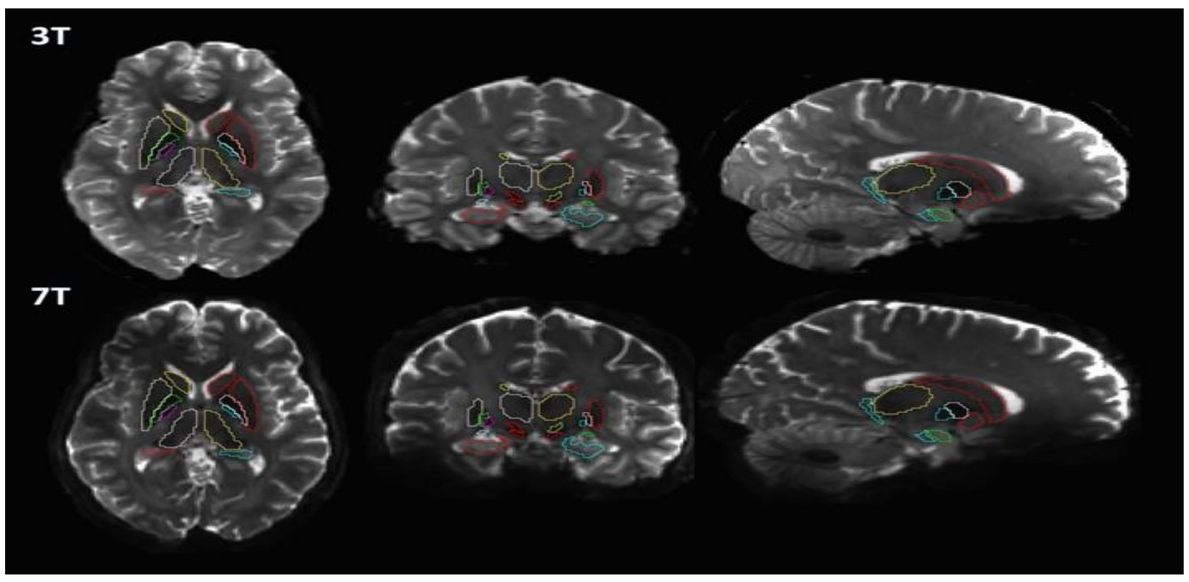

❖ **Figure 3.** Results of 3T and 7T Lead−DBS segmentations of the same subject (HCP Subject ID: 196144) overlaid on 3T and 7T b0 images.

ROI	Mean 3T FA	Mean 7T FA	Student T Test p 3T FA > 7T FA	Mean 3T MD (×10⁻³)	Mean 7T MD (×10⁻³)	Student T Test p 3T MD > 7T MD
Left amygdala	0.189	0.184	0.645	0.748	0.669	0.098
Left caudate	0.164	0.175	0.719	0.679	0.620	0.359
Left globus pallidus externus	0.242	0.189	0.013	0.514	0.424	0.032
Left globus pallidus internus	0.250	0.196	0.597	0.525	0.433	0.890
Left hippocampus	0.168	0.157	0.351	0.788	0.712	0.632
Left nucleus accumbens	0.169	0.149	0.701	0.677	0.659	0.215
Left putamen	0.188	0.175	0.471	0.627	0.569	0.032
Left red nucleus	0.329	0.304	0.332	0.554	0.457	0.394
Left substantia nigra	0.346	0.343	0.001	0.584	0.409	0.006
Left subthalamic nucleus	0.347	0.294	0.030	0.534	0.426	0.635
Left thalamus	0.269	0.248	0.753	0.631	0.583	0.252
Right amygdala	0.169	0.175	0.509	0.757	0.667	0.001
Right caudate	0.177	0.161	0.017	0.677	0.608	0.748
Right globus pallidus externus	0.230	0.250	0.176	0.532	0.384	0.207
Right globus pallidus internus	0.200	0.215	0.070	0.511	0.377	0.162
Right hippocampus	0.169	0.156	0.578	0.767	0.709	0.847
Right nucleus accumbens	0.171	0.147	0.490	0.665	0.642	0.810
Right putamen	0.200	0.186	0.325	0.629	0.546	0.941
Right red nucleus	0.320	0.323	0.357	0.550	0.433	0.082
Right substantia nigra	0.480	0.400	0.743	0.535	0.397	0.001
Right subthalamic nucleus	0.402	0.325	0.692	0.493	0.405	<0.001
Right thalamus	0.272	0.254	0.595	0.636	0.573	0.472
ROI	**Mean 3T AD (×10⁻³)**	**Mean 7T AD (×10⁻³)**	**Student T Test p 3T AD > 7T AD**	**Mean 3T RD (×10⁻³)**	**Mean 7T RD (×10⁻³)**	**Student T Test p 3T RD > 7T RD**
Left amygdala	0.897	0.798	0.084	0.673	0.605	0.126
Left caudate	0.788	0.730	0.400	0.625	0.566	0.343
Left globus pallidus externus	0.636	0.500	0.043	0.452	0.386	0.033
Left globus pallidus internus	0.657	0.513	0.636	0.460	0.393	0.943
Left hippocampus	0.922	0.824	0.570	0.722	0.656	0.742
Left nucleus accumbens	0.788	0.756	0.375	0.621	0.611	0.162
Left putamen	0.751	0.675	0.040	0.565	0.516	0.090
Left red nucleus	0.751	0.605	0.018	0.455	0.383	0.985
Left substantia nigra	0.813	0.568	0.066	0.470	0.329	<0.001
Left subthalamic nucleus	0.717	0.560	0.067	0.442	0.359	0.749
Left thalamus	0.804	0.731	0.873	0.544	0.510	0.159
Right amygdala	0.888	0.789	0.013	0.691	0.607	0.002
Right caudate	0.800	0.708	0.751	0.615	0.559	0.925
Right globus pallidus externus	0.655	0.479	0.477	0.470	0.336	0.186
Right globus pallidus internus	0.612	0.450	0.800	0.460	0.340	0.065
Right hippocampus	0.898	0.821	0.925	0.701	0.654	0.788
Right nucleus accumbens	0.774	0.734	0.872	0.611	0.597	0.603
Right putamen	0.762	0.655	0.537	0.563	0.492	0.743
Right red nucleus	0.738	0.581	0.004	0.456	0.360	0.297
Right substantia nigra	0.850	0.589	0.001	0.377	0.301	0.432
Right subthalamic nucleus	0.711	0.548	<0.001	0.384	0.334	0.037
Right thalamus	0.814	0.721	0.132	0.547	0.498	0.861

❖ **Table 1.** Significant mean differences of 11 subcortical diffusion measures (FA, MD, RD, and AD).

- The left substantia nigra showed significant differences in FA, MD, and RD; the right amygdala showed significant differences in MD and RD; the right red nucleus showed significant differences in AD; and the right substantia nigra and the right subthalamic nucleus showed significant differences in MD and AD.

Discussion

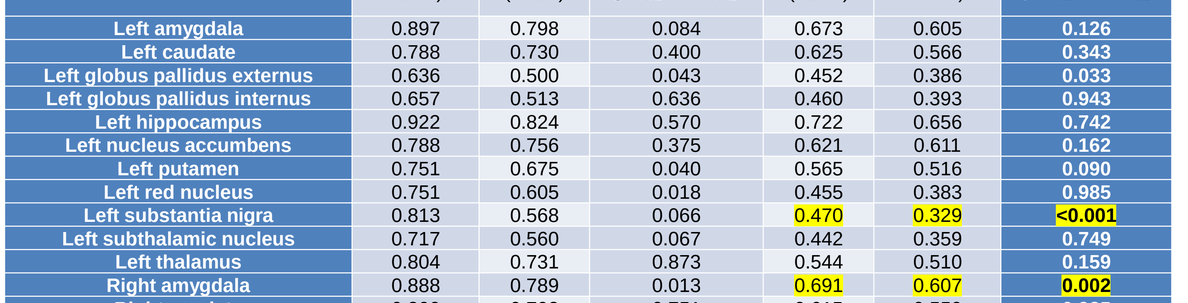

❖ **Figure 4.** Connectivity matrices of significant, FDR−corrected mean differences of diffusion measures, FA, MD, QA, between 3T and 7T connectomes.

- We found that there were significant differences in the left SN, right amygdala, right SN, right RN, and right STN when comparing diffusion measures of 3T and 7T structures.
- In Figure 4, positive values represent higher value of 3T mean diffusion measure while negative values represent higher value of 7T mean diffusion measure.
- Connectivity between ROIs showed more significant increases in FA, MD, and QA in 3T diffusion images when compared with 7T diffusion images.
- 7T were relatively new compared to 3T scanners, meaning that there was little time for the project to experiment with custom hardware or protocols to optimize 7T protocols.
- In the future, improvements to 7T hardware and acquisition protocols should lead to a more accurate representation of a connectome

❖ **Acknowledgments.** This research supported by Basic Science Research Capacity Enhancement Project through Republic of Korea Basic Science Institute (National research Facilities and Equipment Center), grant funded by the Ministry of Education. (grant No. 2021R1A6C101A432)